Singular and Non-singular Path Following Control of a Wheeled Mobile Robot of (2,0) Type

Joanna Płaskonka

Institute of Computer Engineering, Control and Robotics, Wroclaw University of Technology,
Janiszewskiego 11/17, Wroclaw, Poland

Keywords: Path Following, Wheeled Mobile Robot, Serret-Frenet Frame, Nonholonomic Constraints, Model-Based Control.

Abstract: This paper relates to the problem of a path following task for a wheeled mobile platform of (2,0) type. Two kinematic control algorithms, Micaelli-Samson algorithm and Soetanto-Lapierre-Pascoal algorithm, which are based on either the Serret-Frenet frame with an orthogonal projection or the Serret-Frenet frame with a non-orthogonal projection of a robot on the desired path, were presented. The additional condition that should be imposed on the function δ, which is a parameter depending on a linear velocity of the robot and on a distance error, was described. The influence of the function δ on the convergence of the non-singular algorithm has been shown using computer simulations.

1 INTRODUCTION

There are three groups of problems related to a motion control of autonomous vehicles:

- point stabilization,
- trajectory tracking (the robot has to follow a desired curve which is time-parametrized),
- path following (the task of the robot is to follow a curve parametrized by a curvilinear distance from a fixed point).

Various approaches to designing kinematic control strategies for wheeled mobile robots can be used – more general, which could be applied for few types of mobile platforms, and dedicated to particular types of wheeled mobile robots. Better results are usually obtained for the latter ones. The examples of the algorithms dedicated to a certain type of mobile robots may be found e.g. in (Samson, 1992), (De Luca et al., 1998), (Morro et al., 2011), (Płaskonka, 2012). One can also consider a coordinated path following control for a group of wheeled mobile platforms, see e.g. (Xiang et al., 2009), (Ronen and Arogeti, 2012).

Different ideas of describing the position of the robot relative to the path were proposed in the literature. The one, which is the most commonly applied, bases on the Serret-Frenet frame that moves along the desired curve. In this paper two path parametrization approaches are presented. In the first one the Serret-Frenet frame is attached to the point on the path that is closest to the robot, see e.g. (Samson, 1992), (Micaelli and Samson, 1993). Unfortunately such an approach imposes on the vehicle stringent initial conditions constraints. The second approach (Soetanto et al., 2003) does not have such a drawback as the position of the virtual target to be tracked by the robot is defined by a non-orthogonal projection of the vehicle on the path. That approach inspired many scientists, not only those who are focused on control algorithms for mobile platforms, (Indiveri et al., 2007), (Xiang et al., 2009), (Liu et al., 2012).

This paper addresses the problem of the realization of a path following task by a wheeled mobile robot of (2,0) type. The aim of the paper is to present two path following algorithms, Micaelli-Samson algorithm (Micaelli and Samson, 1993) and Soetanto-Lapierre-Pascoal algorithm (Soetanto et al., 2003), and indicate that one should take into account an additional condition related to a function δ, that was introduced in both of the mentioned kinematic control algorithms to broaden the control stability domain, which – to the best of author's knowledge – was not mentioned in the literature so far. In addition, the influence of the function δ on the convergence of Soetanto-Lapierre-Pascoal control algorithm has been presented. The results of additional simulations presenting the influence of values of controller's parameters on the realization of the path following tasks

and simulations taking into account the velocity constraints have been provided as well.

2   MODEL OF A ROBOT

All wheeled mobile robots can be classified into one of five generic types, (Campion et al., 1996). In this paper the considerations will be restricted to a robot belonging to the (2,0) type which is a two-wheel differential-drive robot, also called in the literature a unicycle. In general such a type of a robot consists of a platform equipped with either one or several fixed wheels with a common axle. It might also have a passive caster wheel which serves as a support.

Fig. 1 depicts a unicycle which can be described by generalized coordinates $q = (x, y, \theta)^T$. The point
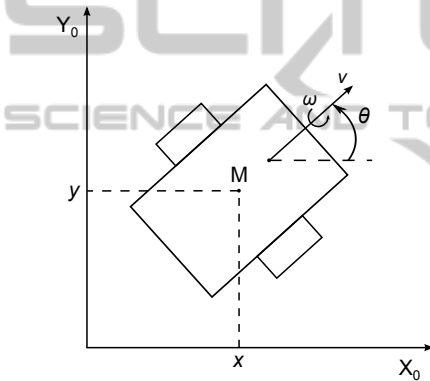

Figure 1: The unicycle's parameters.

M (a robot's guidance point) is located in the middle of the wheel axle of the vehicle. The variables x and y denote the position of the point M relative to the inertial frame, while θ is a robot's orientation. Taking into account the assumptions that the robot's wheels are non-deformable and the robot is moving on a plane without slippage of its wheels, the kinematic model of the considered wheeled mobile robot can be described by the equations

$$\begin{cases} \dot{x} &=& v\cos\theta, \\ \dot{y} &=& v\sin\theta, \\ \dot{\theta} &=& \omega, \end{cases} \tag{1}$$

where symbols v and ω denote unicycle's linear and angular velocities, respectively.

3   DESCRIPTION OF THE ROBOT RELATIVE TO A DESIRED PATH

The position of the robot may be described not only relative to an inertial frame, but also relative to a desired path. For this purpose one may attach to a path the Serret-Frenet frame which in general consists of vectors tangent, normal and binormal to a desired curve. The considered robot is moving on a plane so in that case the Serret-Frenet frame consists only of vectors tangent and normal to the path.

The main difference between a trajectory and a path is that the first one is parametrized by the time, while the latter one is parametrized by a curvilinear distance $s(t)$ from a fixed point, i.e. from the beginning of the path. In other words, a trajectory is a special case of a path when $s(t) = t$. The path P is characterized by a curvature $\kappa(s)$, which is the inversion of the radius of the circle tangent to the path at a point characterized by the parameter s. The desired orientation of the mobile platform satisfies the equation

$$\dot{\theta}_r = \pm\kappa(s)\dot{s}. \tag{2}$$

The sign on the right side of the equation (2) depends on the direction of moving along a desired curve (negative when the Serret-Frenet frame moves in the clockwise direction, positive otherwise).

3.1   The Serret-Frenet Frame with an Orthogonal Projection of a Robot on the Path

In this approach a virtual target to be tracked is defined by the robot's orthogonal projection on the desired path, see Fig. 2. The point M' is the orthogonal
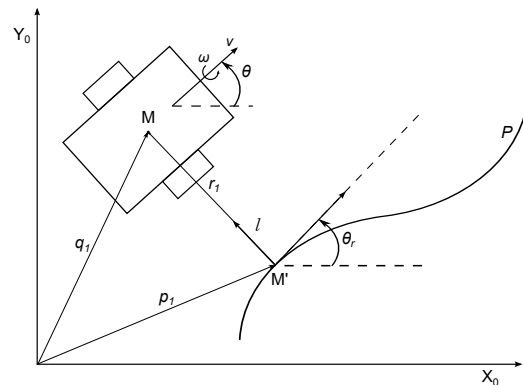

Figure 2: The Serret-Frenet frame definition in a case of an orthogonal projection of a robot on the path.

projection of the point M on the path P and l is the

distance error between the actual vehicle and the virtual one. The relationship between the position of the point M relative to an inertial frame and its position relative to the Serret-Frenet frame can be described by the equation

$$\begin{pmatrix} \mathbf{q_1} \\ 1 \end{pmatrix} = \begin{bmatrix} \mathbf{R}_{\theta_r} & \mathbf{p_1} \\ 0 & 1 \end{bmatrix} \begin{pmatrix} \mathbf{r_1} \\ 1 \end{pmatrix}, \qquad (3)$$

where

$$\mathbf{R}_{\theta_r} = \mathbf{R} = \mathbf{Rot}(z, \theta_r) = \begin{bmatrix} \cos\theta_r & -\sin\theta_r & 0 \\ \sin\theta_r & \cos\theta_r & 0 \\ 0 & 0 & 1 \end{bmatrix}. \qquad (4)$$

After differentiating and transforming the equation (3), one has

$$\dot{\mathbf{r}}_1 = \mathbf{R}^T \dot{\mathbf{q}}_1 - \mathbf{R}^T \dot{\mathbf{R}} \mathbf{r_1} - \mathbf{R}^T \dot{\mathbf{p}}_1. \qquad (5)$$

Using the relationships

$$\mathbf{r_1} = (0 \quad l \quad 0)^T, \qquad (6)$$

$$\mathbf{q_1} = (x \quad y \quad 0)^T \qquad (7)$$

and

$$\mathbf{v_B} = \dot{\mathbf{R}}^T \dot{\mathbf{p}}_1 = (\dot{s} \quad 0 \quad 0)^T, \qquad (8)$$

as the reference vehicle is moving along a desired path in the direction of X axis of the Serret-Frenet frame, the equation (5) can be rewritten as

$$\begin{pmatrix} 0 \\ \dot{l} \\ 0 \end{pmatrix} = \begin{bmatrix} \cos\theta_r & \sin\theta_r & 0 \\ -\sin\theta_r & \cos\theta_r & 0 \\ 0 & 0 & 1 \end{bmatrix} \begin{pmatrix} \dot{x} \\ \dot{y} \\ 0 \end{pmatrix} + $$
$$- \begin{bmatrix} 0 & -\dot{\theta}_r & 0 \\ \dot{\theta}_r & 0 & 0 \\ 0 & 0 & 0 \end{bmatrix} \begin{pmatrix} 0 \\ l \\ 0 \end{pmatrix} - \begin{pmatrix} \dot{s} \\ 0 \\ 0 \end{pmatrix}, (9)$$

which leads to

$$\dot{l} = (-\sin\theta_r \quad \cos\theta_r) \begin{pmatrix} \dot{x} \\ \dot{y} \end{pmatrix}, \qquad (10)$$

$$\dot{s} = \frac{(\cos\theta_r \quad \sin\theta_r)}{1 \mp \kappa(s)l} \begin{pmatrix} \dot{x} \\ \dot{y} \end{pmatrix}. \qquad (11)$$

To avoid singularity $l = \pm\frac{1}{\kappa(s)}$ one has to ensure that during the control process an inequality $|l\kappa(s)| < 1$ holds, which means that the parametrization is local. In addition, one can determine the orientation error

$$\tilde{\theta} = \theta - \theta_r \qquad (12)$$

and its derivative

$$\dot{\tilde{\theta}} = \dot{\theta} - \dot{\theta}_r = \dot{\theta} \mp \kappa(s)\dot{s}. \qquad (13)$$

Finally the kinematic model of a wheeled mobile robot of (2,0) type derived with respect to Serret-Frenet frame can be described by the following system of equations

$$\begin{cases} \dot{l} &= v\sin\tilde{\theta}, \\ \dot{s} &= \frac{v\cos\tilde{\theta}}{1\mp\kappa(s)l}, \\ \dot{\tilde{\theta}} &= \omega \mp \frac{\kappa(s)v\cos\tilde{\theta}}{1\mp\kappa(s)l}. \end{cases} \qquad (14)$$

3.2 The Serret-Frenet Frame with a Non-orthogonal Projection of a Robot on the Path

The methodology described in this subsection avoids the occurrence of the singularities which are present in control strategies based on the approach presented in subsection 3.1. This is done by using the Serret-Frenet frame which is not attached to the point on the path that is closest to the vehicle, see Fig. 3. As a result one has to take into account an extra controller design parameter. In that situation there are three path following errors – an orientation error $\tilde{\theta}$ and two distance errors, s_1 in the direction of the X axis and y_1 in the direction of Y axis of the Serret-Frenet frame. Such an approach was proposed in (Soetanto et al., 2003).
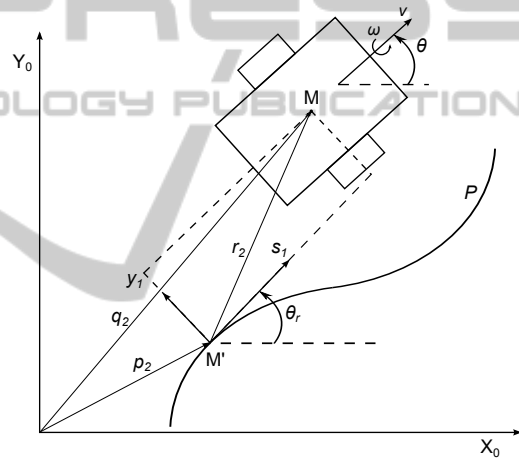
Figure 3: The Serret-Frenet frame definition in a case of a non-orthogonal projection of a robot on the path.

The velocity of $\mathbf{r_2}$ is equal to

$$\dot{\mathbf{r}}_2 = \mathbf{R}^T \dot{\mathbf{q}}_2 - \mathbf{R}^T \dot{\mathbf{R}} \mathbf{r_2} - \mathbf{R}^T \dot{\mathbf{p}}_2 \qquad (15)$$

with

$$\mathbf{r_2} = (s_1 \quad y_1 \quad 0)^T, \qquad (16)$$

$$\mathbf{q_2} = (x \quad y \quad 0)^T \qquad (17)$$

and

$$\dot{\mathbf{R}}^T \dot{\mathbf{p}}_2 = (\dot{s} \quad 0 \quad 0)^T. \qquad (18)$$

From (15) one gets

$$\begin{pmatrix} \dot{s}_1 \\ \dot{y}_1 \\ 0 \end{pmatrix} = \begin{bmatrix} \cos\theta_r & \sin\theta_r & 0 \\ -\sin\theta_r & \cos\theta_r & 0 \\ 0 & 0 & 1 \end{bmatrix} \begin{pmatrix} \dot{x} \\ \dot{y} \\ 0 \end{pmatrix} + $$
$$- \begin{bmatrix} 0 & -\dot{\theta}_r & 0 \\ \dot{\theta}_r & 0 & 0 \\ 0 & 0 & 0 \end{bmatrix} \begin{pmatrix} s_1 \\ y_1 \\ 0 \end{pmatrix} - \begin{pmatrix} \dot{s} \\ 0 \\ 0 \end{pmatrix} (19)$$

and thus

$$\dot{s}_1 = \begin{pmatrix} \cos\theta_r & \sin\theta_r \end{pmatrix} \begin{pmatrix} \dot{x} \\ \dot{y} \end{pmatrix} - \dot{s}(1 - y_1\kappa(s)), \quad (20)$$

$$\dot{y}_1 = \begin{pmatrix} -\sin\theta_r & \cos\theta_r \end{pmatrix} \begin{pmatrix} \dot{x} \\ \dot{y} \end{pmatrix} - \dot{s}\kappa(s)s_1. \quad (21)$$

There is no singularity related to distance errors in equations (20)-(21). For the unicycle the kinematic model expressed with respect to the Serret-Frenet frame with a non-orthogonal projection of a robot on the path is given by the following equations

$$\begin{cases} \dot{s}_1 &= -\dot{s}(1 - \kappa(s)y_1) + v\cos\tilde{\theta}, \\ \dot{y}_1 &= -\kappa(s)\dot{s}s_1 + v\sin\tilde{\theta}, \\ \dot{\tilde{\theta}} &= \omega \mp \kappa(s)\dot{s}. \end{cases} \quad (22)$$

4 PATH FOLLOWING ALGORITHMS

The considered control problem is to design a kinematic control law such that the wheeled mobile robot of (2,0) type follows a desired path and path following errors converge to zero. The desired path has to be admissible, i.e. it can be realized without slippage of robot's wheels.

It is assumed that a direction of a movement along the desired curve is opposite to the clockwise direction, this means that

$$\dot{\tilde{\theta}} = \kappa(s)\dot{s}. \quad (23)$$

Hence the equations describing path following errors for a case of an orthogonal projection of a robot on the path have a form as below

$$\begin{cases} \dot{l} &= v\sin\tilde{\theta}, \\ \dot{\tilde{\theta}} &= \omega - \frac{\kappa(s)v\cos\tilde{\theta}}{1 - \kappa(s)l}. \end{cases} \quad (24)$$

and in a case of a non-orthogonal projection are equal to

$$\begin{cases} \dot{s}_1 &= -\dot{s}(1 - \kappa(s)y_1) + v\cos\tilde{\theta}, \\ \dot{y}_1 &= -\kappa(s)\dot{s}s_1 + v\sin\tilde{\theta}, \\ \dot{\tilde{\theta}} &= \omega - \kappa(s)\dot{s}. \end{cases} \quad (25)$$

4.1 Singular Control Algorithm

Micaelli-Samson kinematic control law (Micaelli and Samson, 1993) for the system (24) is equal to

$$\begin{aligned} \omega &= \frac{\kappa(s)v\cos\tilde{\theta}}{1 - \kappa(s)l} + \frac{\partial\delta(l,v)}{\partial l}v\sin\tilde{\theta} + \frac{\partial\delta(l,v)}{\partial v}\dot{v} + \\ &\quad - \lambda_{\tilde{\theta}}\left[f\frac{\partial f}{\partial l}v\frac{\sin\tilde{\theta} - \sin\delta(l,v)}{\tilde{\theta} - \delta(l,v)} - k|v|(\tilde{\theta} - \delta(l,v))\right], \\ &\quad k > 0, \quad \lambda_{\tilde{\theta}} > 0, \end{aligned} \quad (26)$$

where $v(t)$ and $\dot{v}(t)$ are bounded, $v(t)$ does not tend to zero when t tends to infinity, the functions

$$f(l) : (-r, r) \to R$$

and

$$\delta(l, v) : R \times R \to R$$

are C^2 and C^1 respectively and the following conditions are satisfied:

- $f(\pm r) = \pm\infty$,
- $f(0) = \delta(0, v) = 0$,
- $\frac{\partial f}{\partial l}(l) > 0, \forall l$,
- $vf(l)\sin\delta(l, v) \leq 0, \forall l, \forall v$.

The function δ was introduced to set the desired values for the orientation error $\tilde{\theta}$ during transients. What is more, the following inequality should hold

$$|\delta(l, v)| < \frac{\pi}{2}, \quad \forall l, \forall v. \quad (27)$$

The system (24) with a closed-loop of the feedback signal (26) is asymptotically stable. In addition, if $f(l)$ tends to infinity when l tends to $\frac{1}{\kappa_{max}}$, it is possible to keep $l(t)$ in the open interval $\left(-\frac{1}{\kappa_{max}}, \frac{1}{\kappa_{max}}\right)$ when $l(0)$ belongs to this interval.

Proof. Consider the Lyapunov function

$$V_1 = \frac{1}{2}\left[f^2(l) + \frac{1}{\lambda_{\tilde{\theta}}}(\tilde{\theta} - \delta(l, v))^2\right]. \quad (28)$$

The time-derivative of V_1

$$\begin{aligned} \dot{V}_1 &= f\frac{\partial f}{\partial l}\dot{l} + \frac{1}{\lambda_{\tilde{\theta}}}(\tilde{\theta} - \delta)(\dot{\tilde{\theta}} - \dot{\delta}) = \\ &= f\frac{\partial f}{\partial l}v\sin\delta + (\tilde{\theta} - \delta)[\frac{1}{\lambda_{\tilde{\theta}}}(\omega + \\ &\quad - \frac{\kappa(s)v\cos\tilde{\theta}}{1 - \kappa(s)l} - \frac{\partial\delta}{\partial l}v\sin\tilde{\theta} - \frac{\partial\delta}{\partial v}\dot{v}) + \\ &\quad + f\frac{\partial f}{\partial l}v\frac{\sin\tilde{\theta} - \sin\delta}{\tilde{\theta} - \delta}] = \\ &= f\frac{\partial f}{\partial l}v\sin\delta - k|v|(\tilde{\theta} - \delta)^2 \end{aligned} \quad (29)$$

is non-positive. This means that $\lim_{t\to\infty} V_1(t) = V_{1lim}$ and $f(l)$ and $(\tilde{\theta} - \delta)$ are bounded. $\dot{V}_1$ is uniformly continuous because its derivative is bounded as sum of bounded functions. By Barbalat's lemma $\dot{V}_1$ tends to zero. Therefore $f\frac{\partial f}{\partial l}v\sin\delta \to 0$ and $v(\tilde{\theta} - \delta) \to 0$. Differentiating $(\tilde{\theta} - \delta)$ with respect to time gives

$$\begin{aligned} \frac{d}{dt}(\tilde{\theta} - \delta) &= -\lambda_{\tilde{\theta}}f\frac{\partial f}{\partial l}v\frac{\sin\tilde{\theta} - \sin\delta}{\tilde{\theta} - \delta} + \\ &\quad - k\lambda_{\tilde{\theta}}|v|(\tilde{\theta} - \delta). \end{aligned} \quad (30)$$

Hence

$$\begin{aligned} \frac{d}{dt}[v^2(\tilde{\theta} - \delta)] &= 2v\dot{v}(\tilde{\theta} - \delta) - \lambda_{\tilde{\theta}}f\frac{\partial f}{\partial l}v^3\frac{\sin\tilde{\theta} - \sin\delta}{\tilde{\theta} - \delta} + \\ &\quad - k\lambda_{\tilde{\theta}}|v|v^2(\tilde{\theta} - \delta) \end{aligned} \quad (31)$$

is the sum of two terms which tend to zero and third term which is uniformly continuous. As $v^2(\tilde\theta - \delta)$ tends to zero, the extension of Barbalat's lemma (Micaelli and Samson, 1993) tells us that $\frac{d}{dt}[v^2(\tilde\theta - \delta)]$ also tends to zero which implies that the term $\lambda_{\tilde\theta} f \frac{\partial f}{\partial l} v^3 \frac{\sin\tilde\theta - \sin\delta}{\tilde\theta - \delta} \to 0$. The expression $\frac{\sin\tilde\theta - \sin\delta}{\tilde\theta - \delta}$ requires a special comment. It can be rewritten in the following way

$$\frac{\sin\tilde\theta - \sin\delta}{\tilde\theta - \delta} = \frac{\sin\frac{\tilde\theta - \delta}{2}\cos\frac{\tilde\theta + \delta}{2}}{\frac{\tilde\theta - \delta}{2}} \qquad (32)$$

which for $(\tilde\theta - \delta) \to 0$ tends to $\cos\delta$ or one can also notice that for $(\tilde\theta - \delta) \to 0$ the expression $\frac{\sin\tilde\theta - \sin\delta}{\tilde\theta - \delta}$ is equal to the derivative of the sine function. If only δ does not tend to $\frac{m\pi}{2}$, $m \in Z$, the the whole term $\frac{\sin\tilde\theta - \sin\delta}{\tilde\theta - \delta}$ does not tend to zero. This fact was not indicated in (Micaelli and Samson, 1993). It seems reasonable to assume that δ should be less than $\frac{\pi}{2}$ for all l and for all v. Under this assumption $f\frac{\partial f}{\partial l}v$ tends to zero. At the beginning it was assumed that $\frac{\partial f}{\partial l}(l) > 0$ which leads to $vf \to 0$. Using the facts that $v(\tilde\theta - \delta) \to 0$ and $vf \to 0$, one may conclude that $v^2 V_1$ tends to zero and $V_{1lim} = 0$. Thus both f and $(\tilde\theta - \delta)$ tend to zero. From the properties of the function f, l also tends to zero and therefore $\delta \to 0$. Finally one conclude that $\tilde\theta$ tends to zero which completes the proof. $\qquad \square$

4.2 Non-singular Control Algorithm

The control algorithm proposed in (Soetanto et al., 2003) for the system (25) is equal to

$$\begin{aligned}
\dot{s} &= v\cos\tilde\theta + k_1 s_1, \\
\omega &= \kappa(s)\dot{s} + \dot\delta(y_1, v) - \gamma y_1 v \frac{\sin\tilde\theta - \sin\delta(y_1, v)}{\tilde\theta - \delta(y_1, v)} + \\
&\quad - k_2(\tilde\theta - \delta(y_1, v)), \\
&\quad k_1, k_2 > 0, \quad \gamma = const,
\end{aligned} \qquad (33)$$

where the following assumptions have been made

- $\lim_{t\to\infty} v(t) \neq 0$, e.g. $v = const$,
- $\delta(0, v) = 0$,
- $\forall_{y_1}\forall_v \, y_1 v \sin\delta(y_1, v) \leq 0$.

What is more, the following inequality should hold

$$|\delta(y_1, v)| < \frac{\pi}{2}, \quad \forall y_1, \forall v, \qquad (34)$$

which was not mentioned in (Soetanto et al., 2003). The control algorithm guarantees the convergence of y_1, s_1 and $\tilde\theta$ to zero. That can be shown using the following Lyapunov function

$$V_2 = \frac{1}{2}(s_1^2 + y_1^2) + \frac{1}{2\gamma}(\tilde\theta - \delta(y_1, v))^2 \qquad (35)$$

and carrying out the similar reasoning to one which was presented in the subsection 4.1. The complete proof of the convergence can be found in (Płaskonka, 2013).

5 SIMULATION RESULTS

The simulations were carried out to illustrate the behaviour of the wheeled mobile robot of (2,0) type with the non-singular Soetanto-Lapierre-Pascoal controller. The initial position of the platform was equal to $(x_0, y_0, \theta_0) = (12, 2, \frac{\pi}{4})$. The desired path was the circle described by the equations

$$\begin{aligned}
x(s) &= R\cos\left(\frac{s}{R}\right), \\
y(s) &= R\sin\left(\frac{s}{R}\right),
\end{aligned}$$

where $R = 2$ m.

5.1 The Influence of Different Values of δ Function on the Realization of the Task

Parameters of the kinematic controller were set to the values presented below:

- $v = 1$,
- $k_1 = 1$,
- $k_2 = 1000$,
- $\gamma = 1$,
- $\theta_a = \{\frac{\pi}{4}, \frac{\pi}{2}, \pi, 2\pi\}$,
- $\delta = -\text{sign}(v)\theta_a \tanh y_1$.

The results of the simulations were presented in Fig. 4-11.
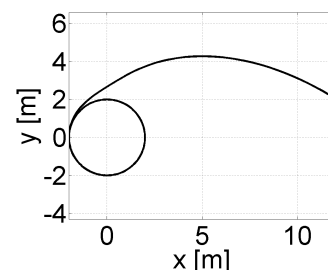

Figure 4: The path following for the unicycle, XY plot (Soetanto-Lapierre-Pascoal algorithm, $\theta_a = \frac{\pi}{4}$).
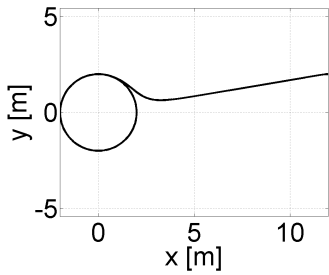
Figure 5: The path following for the unicycle, XY plot (Soetanto-Lapierre-Pascoal algorithm, $\theta_a = \frac{\pi}{2}$).
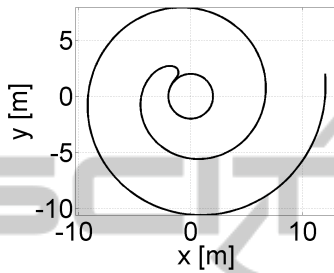

Figure 6: The path following for the unicycle, XY plot (Soetanto-Lapierre-Pascoal algorithm, $\theta_a = \pi$).
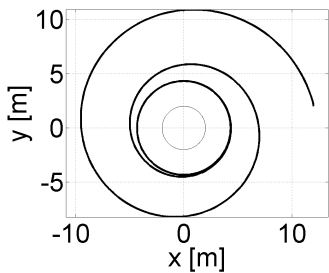

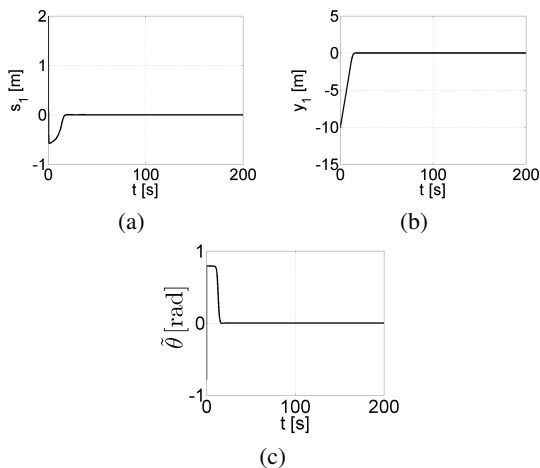Figure 7: The path following for the unicycle, XY plot (Soetanto-Lapierre-Pascoal algorithm, $\theta_a = 2\pi$).

Figure 8: The path following for the unicycle (Soetanto-Lapierre-Pascoal algorithm, $\theta_a = \frac{\pi}{4}$): (a) the distance error s_1, (b) the distance error y_1, (c) the orientation error $\tilde{\theta}$.
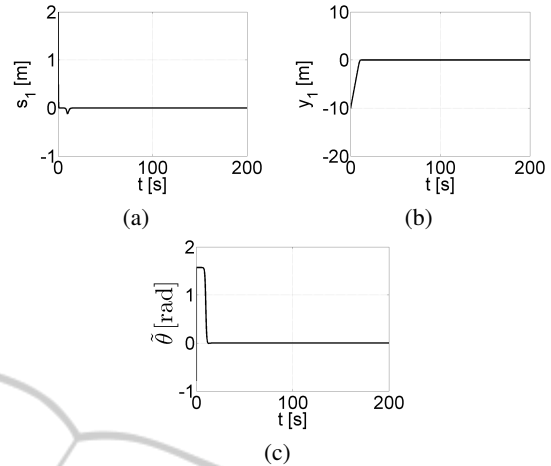

Figure 9: The path following for the unicycle (Soetanto-Lapierre-Pascoal algorithm, $\theta_a = \frac{\pi}{2}$): (a) the distance error s_1, (b) the distance error y_1, (c) the orientation error $\tilde{\theta}$.
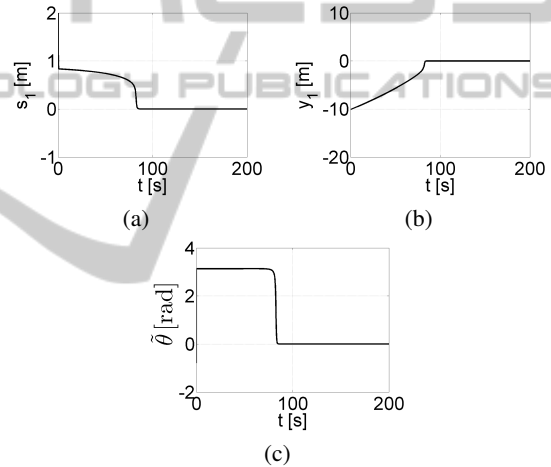

Figure 10: The path following for the unicycle (Soetanto-Lapierre-Pascoal algorithm, $\theta_a = \pi$): (a) the distance error s_1, (b) the distance error y_1, (c) the orientation error $\tilde{\theta}$.

5.2 The Influence of Different Values of k_i Parameters on the Realization of the Task

Parameters of the kinematic controller were set to the values presented below:

- $v = 1$,
- $k_1 = \{0.1, 1, 10, 100, 1000, 10000\}$,
- $k_2 = \{0.1, 1, 10, 100, 1000, 10000\}$,
- $\gamma = 1$,
- $\theta_a = \frac{\pi}{4}$,
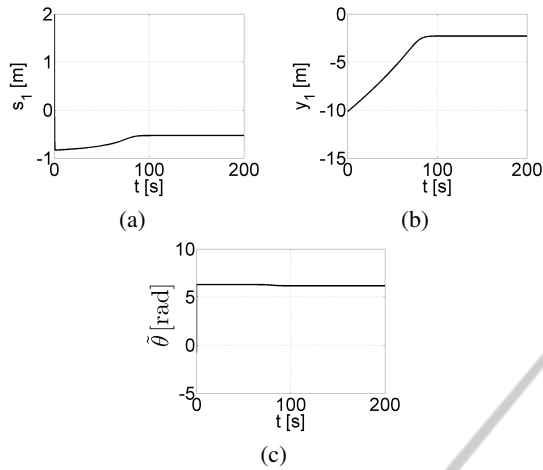- $\delta = -\text{sign}(v)\theta_a \tanh y_1$.

(a)

(b)

(c)

Figure 11: The path following for the unicycle (Soetanto-Lapierre-Pascoal algorithm, $\theta_a = 2\pi$): (a) the distance error s_1, (b) the distance error y_1, (c) the orientation error $\tilde{\theta}$.

The chosen quality indicator for the presented algorithm is equal to

$$Q = \sum_{k=1}^{3} I_k + \sum_{j=1}^{2} \int_0^T u_j^2,$$

where $I_1 = \int_0^T s_1^2\, dt$, $I_2 = \int_0^T y_1^2\, dt$, $I_3 = \int_0^T \tilde{\theta}^2\, dt$ and u_1, u_2 are control inputs. Table 1 presents values of Q for selected values of the control parameters k_i. The quality indicator reached the minimum for $k_1 = 1$ and $k_2 = 10$. The results of the simulations for those parameters were presented in Fig. 12-13.
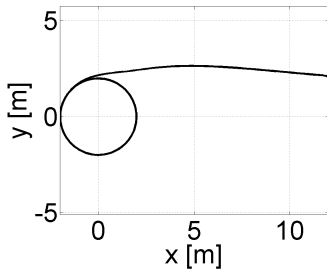

Figure 12: The path following for the unicycle, XY plot (Soetanto-Lapierre-Pascoal algorithm, $k_1 = 1$, $k_2 = 10$).

5.3 The Simulations Taking into Account Velocity Constraints

Parameters of the kinematic controller were set to the values presented below:

- $v = 1$,
- $k_1 = 1$,
- $k_2 = 10$,
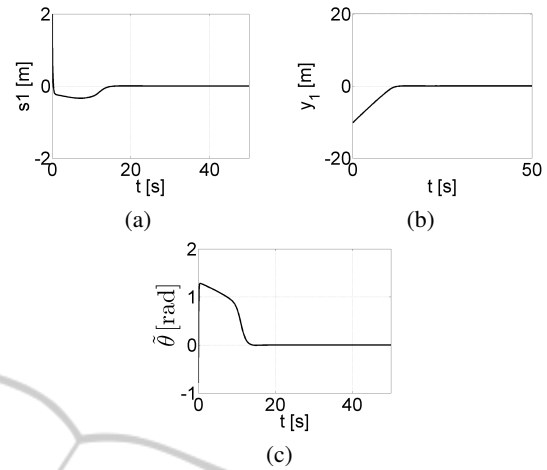- $\gamma = 1$,

(a)

(b)

(c)

Figure 13: The path following for the unicycle (Soetanto-Lapierre-Pascoal algorithm, $k_1 = 1$, $k_2 = 10$): (a) the distance error s_1, (b) the distance error y_1, (c) the orientation error $\tilde{\theta}$.

- $\theta_a = \frac{\pi}{4}$,
- $\delta = -\text{sign}(v)\theta_a \tanh y_1$.

The velocity constraint imposed on the on the robot is chosen as $-\frac{\pi}{5} \leq \omega \leq \frac{\pi}{5}$ [rad/s]. The results of the simulations were presented in Fig. 14-15.
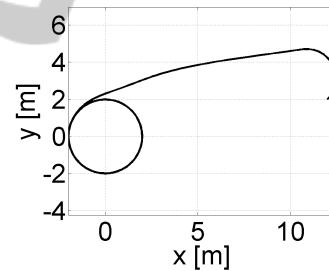

Figure 14: The path following for the unicycle, XY plot (Soetanto-Lapierre-Pascoal algorithm, simulations taking into account velocity constraints).

6 CONCLUSIONS

In the paper singular and non-singular kinematic path following controllers have been presented. It was suggested to take into account an additional condition imposed on the function δ which is a parameter of both algorithms. According to that condition the values of δ should be smaller than $\frac{\pi}{2}$. The simulations of the Soetanto-Lapierre-Pascoal algorithm have shown that it is reasonable to limit values of δ. For $\theta_a > \frac{\pi}{2}$ the convergence of the algorithm was unacceptably slow. Simulation analysis has shown that the presented algorithm works properly for different values of the k_i

Table 1: The values of the quality indicator Q obtained in the simulations for selected values of k_i parameters.

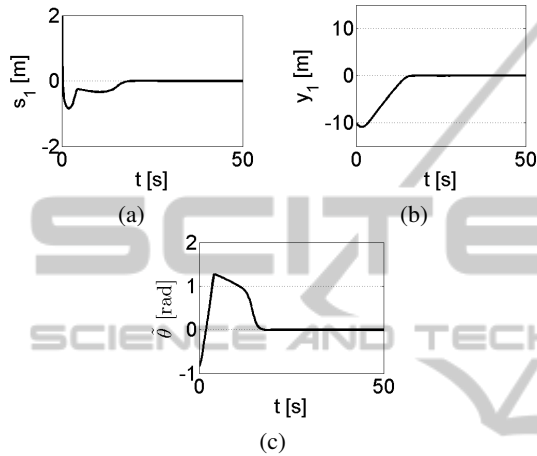| k_1	k_2					
	0.1	**1**	**10**	**100**	**1000**	**10 000**
0.1	631.9	513.2	512.4	681.9	1 801.3	12 835.6
1	607.3	514.2	490.1	664.3	1 789.1	12 824.1
10	626.3	518.7	497.5	699.0	1 836.5	12 873.4
100	635.9	526.5	506.1	734.4	2 013.2	13 148.5
1000	710.4	600.8	580.5	815.6	2 339.1	14 886.6
10 000	1 438.4	1 328.3	1 307.9	1 543.8	3 131.6	18 164.1

Figure 15: The path following for the unicycle (Soetanto-Lapierre-Pascoal algorithm, simulations taking into account velocity constraints): (a) the distance error s_1, (b) the distance error y_1, (c) the orientation error $\tilde{\theta}$.

parameters, however choosing large values of the controller's parameters is undesirable due to a significant control cost. What is more, the path following task is realized correctly by the considered wheeled mobile robot when the Soetanto-Lapierre-Pascoal algorithm is modified by adding velocity constraints.

An extension of this work could be testing if the other kinds of δ function, not necessarily sigmoid-like, could be applied for the presented algorithms.

REFERENCES

Campion, G., Bastin, G., and d'Andréa Novel, B. (1996). Structural properties and classification of kinematic and dynamic models of wheeled mobile robots. *IEEE Transactions on Robotics and Automation*, 12(5):47–61.

De Luca, A., Oriolo, G., and Samson, C. (1998). Feedback control of a nonholonomic car-like robot. In Laumond, J.-P., editor, *Robot Motion Planning and Control*, pages 171–253. Springer-Verlag.

Indiveri, G., Nuchter, A., and Lingemann, K. (2007). High speed differential drive mobile robot path following control with bounded wheel speed commands. *Proceedings of the 2007 IEEE International Conference on Robotics and Automation*, pages 2202–2207.

Liu, C., McAree, O., and Chen, W.-H. (2012). Path following for small UAVs in the presence of wind disturbance. *Proceedings of the UKACC International Conference on Control*, pages 613–618.

Micaelli, A. and Samson, C. (1993). Trajectory tracking for unicycle-type and two-steering-wheels mobile robots. *Technical Report No. 2097, INRIA, Sophia-Antipolis, France*.

Morro, A., Sgorbissa, A., and Zaccaria, R. (2011). Path following for unicycle robots with an arbitrary path curvature. *IEEE Transactions on Robotics*, 27(5):1016–1023.

Płaskonka, J. (2012). The path following control of a unicycle based on the chained form of a kinematic model derived with respect to the Serret-Frenet frame. *Proceedings of 17th International Conference on Methods and Models in Automation & Robotics, MMAR 2012*, 27(5):1016–1023.

Płaskonka, J. (2013). Different kinematic path following controllers for a wheeled mobile robot of (2,0) type. *Sent for publication*.

Ronen, R. and Arogeti, S. (2012). Coordinated path following control for a group of car-like vehicles. *Proceedings of the IEEE 12th International Conference on Control, Automation, Robotics & Vision*, pages 719–724.

Samson, C. (1992). Path following and time-varying feedback stabilization of a wheeled mobile robots. *Proceedings of the IEEE Int. Conf. on Advanced Robotics and Computer Vision*, pages 1.1–1.5.

Soetanto, D., Lapierre, L., and Pascoal, A. (2003). Adaptive, non-singular path-following control of dynamic wheeled robots. *Proceedings of the IEEE Conference on Decision and Control*, 2:1765–1770.

Xiang, X., Lapierre, L., Jouvencel, B., and Parodi, O. (2009). Coordinated path following control of multiple wheeled mobile robots through decentralized speed adaptation. *Proceedings of the IEEE/RSJ International Conference on Intelligent Robots and Systems*, pages 4547–4552.